

First-principles study of magnetic properties of L1₀-ordered MnPt and FePt alloys

Zhihong Lu, Roman V. Chepulskii,^{*} and W. H. Butler[†]

Center for Materials for Information Technology, University of Alabama, Tuscaloosa, Alabama 35487, USA

(Received 18 January 2010; revised manuscript received 9 March 2010; published 30 March 2010)

Using first-principles methods, we study the magnetic and electronic properties of three different spin configurations of the L1₀ phase of FePt and MnPt alloys. It is found that MnPt and FePt may be approximately considered as magnetic antipodes with opposite ferromagnetic (FM)—antiferromagnetic (AFM) and in-plane/out-of-plane magnetocrystalline anisotropy (MCA) relationships. In MnPt, the most stable phase is the AFM configuration with AFM chessboard spin coupling in the (001) plane, FM spin coupling between (001) planes, and all spin directions aligned in the (001) plane. Whereas in FePt, the most stable is the FM configuration with all spin directions aligned perpendicular to (001) plane. The out-of-plane MCA of MnPt is more than an order of magnitude less (~ 0.1 meV) than that of FePt (~ 2.9 meV) in their corresponding magnetic ground states. Our calculations indicate that an AFM state can be achieved in FePt by a small variation in tetragonality ratio (from 0.98 to 0.94). A pseudogap is observed at the Fermi energy for MnPt and just below the Fermi energy for FePt for the chessboard AFM model. This pseudogap may explain the ground-state magnetic configuration of MnPt.

DOI: 10.1103/PhysRevB.81.094437

PACS number(s): 75.30.Gw, 71.20.Lp, 75.50.Ee, 75.50.Ss

I. INTRODUCTION

In recent years, MnPt and FePt alloys have been intensively studied. The antiferromagnet (AFM), MnPt, is an important material for magnetic recording and other spintronic applications such as magnetic random-access memory because it can be used as a pinning layer in giant magnetoresistive and tunneling magnetoresistive devices.¹⁻³ The ferromagnet (FM), FePt, is a promising medium material for high-density magnetic recording⁴⁻⁶ because its high magnetocrystalline anisotropy suppresses superparamagnetism in nanoscale particles and elements.

At low temperatures, both MnPt and FePt are observed⁷ to have the layered L1₀ (CuAu) atomic structure (see Fig. 1) with small tetragonal distortions. At room temperature, MnPt is found experimentally⁸⁻¹¹ to have antiferromagnetic order with antiferromagnetic coupling between adjacent Mn atoms in the (001) plane at distance $a/\sqrt{2}$ and ferromagnetic coupling between two adjacent Mn atoms in the [001] direction

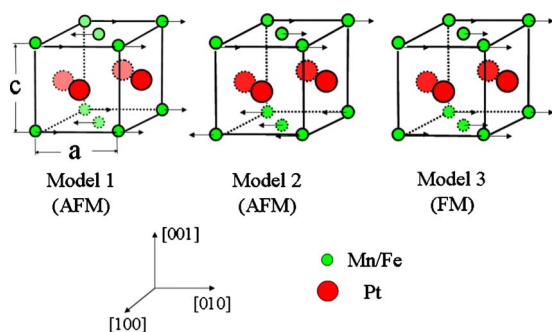


FIG. 1. (Color online) Two antiferromagnetic (Model 1,2) and one ferromagnetic (Model 3) configurations of fully L1₀-ordered equiatomic MnPt and FePt alloys considered in the present study. The arrows indicate the relative directions of Mn or Fe magnetic moments with respect to each other (rather than to crystallographic directions). The Pt magnetic moments are not indicated because they are found to be considerably smaller than those of Fe and Mn.

at distance c (see Model 1 in Fig. 1). However, the general direction of atom magnetic moments with respect to the lattice is reported to be both composition^{8,9} and temperature^{9,11} dependent with some controversial results. Moreover, a ferromagnetic phase is found in quenched MnPt samples with partially ordered and disordered Mn and Pt atoms^{8,12} and in sputtered disordered samples.¹³ Most previous studies of MnPt have been experimental and have mainly focused on the phenomenon of exchange bias in which a MnPt layer is used to shift the hysteresis curve of an adjacent ferromagnetic layer.^{14,15} To our knowledge, a theoretical study of the magnetic properties of MnPt and of possible phase competition in MnPt is still lacking.

Experimentally, FePt is well known to be ferromagnetic at room temperature¹⁶ with a very large anisotropy energy (1.2 meV/f.u. for bulk) perpendicular to the atomic planes of Fe and Pt.^{17,18} However, the calculations of Brown *et al.*¹⁹ claim that there is a competition between ferromagnetism and antiferromagnetism in FePt: FM becomes energetically favorable compared to AFM as tetragonality and/or L1₀ order decreases (so, effectively, as the system becomes more cubic).

Since FePt and MnPt both have L1₀ structures, the only difference between them is that the Fe atom has one more electron than the Mn atom. However, they have different equilibrium magnetic states. In this paper, we report a systematic study and comparison of the magnetic and electronic properties of MnPt and FePt L1₀-ordered alloys with different magnetic configurations. Such a study may help us to understand the reasons behind their very different magnetic properties.

II. COMPUTATION DETAILS

We consider two collinear antiferromagnetic configurations and one collinear ferromagnetic configuration of fully L1₀-ordered equiatomic MnPt and FePt alloys (see Fig. 1). All energies are calculated from first principles within the generalized gradient approximation (GGA) to density-

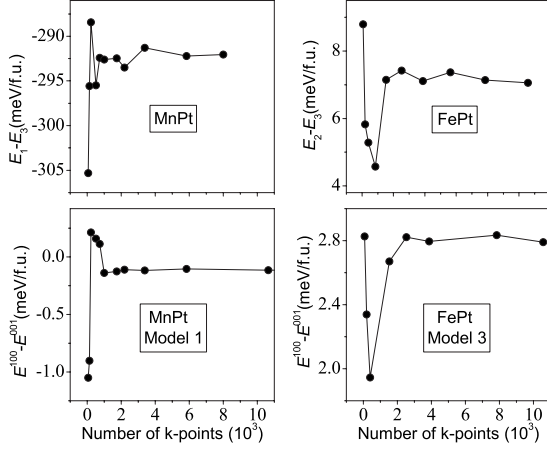


FIG. 2. Convergence of energy differences with respect to number of k -points in the first Brillouin zone. E_i is the energy of i th model (neglecting spin-orbit coupling). $E^{[lmn]}$ is the energy of the corresponding model with all magnetic moments being parallel to $[lmn]$ direction (including spin-orbit coupling).

functional theory (DFT) with the use of projector augmented waves pseudopotentials and exchange-correlation functionals as parameterized by Perdew and Wang²⁰ and implemented within the VASP (Ref. 21) program package. All structures are fully relaxed including shape (if tetragonality is not fixed) and volume of the cell. All calculated energy values are presented per $L1_0$ formula unit (f.u.) cell, which consists of one Fe or Mn and one Pt atoms.

In evaluating small energy differences between atomic configurations and typically even smaller differences be-

tween magnetic configurations, it is important to use enough k -points to sample the reciprocal space with sufficient accuracy. Analyzing the k -point convergence (see Fig. 2), we find that 2000 k -points in the first Brillouin zone are sufficient for accurate estimation of energy differences between the three considered models for MnPt and FePt. We use an energy cutoff of 270 eV. We also find that 5000 and 3000 k -points are sufficient for accurate estimation of magnetocrystalline anisotropy (MCA) energy of MnPt and FePt, respectively, in all three considered models. Note that, in all considered cases, we find that the spin-orbit coupling has a tiny effect on the energy differences (less than 3 meV/f.u.) and magnetic moments. Thus, the spin-orbit coupling is taken into account only for calculations of MCA. Atomic-site-projected (spin) magnetic moments are determined by integrating the magnetization within Wigner-Seitz atomic spheres. There is some ambiguity in the calculated atomic moments per atom arising from the ambiguity of dividing space among the atoms. We have attempted to reduce that ambiguity by choosing Wigner-Seitz sphere radii such that the total volume of the spheres is the same as the cell volume.

III. GROUND STATES

The results of our first-principles calculations for all three models in MnPt and FePt alloys are shown in Table I and Fig. 3. We conclude that, under a complete relaxation, Model 1 (AFM) and Model 3 (FM) are the ground states in MnPt and FePt, respectively. Such results are in agreement with experimental observations.^{8–11,16–18} The small (~ 7 meV) energetic preference of FM over AFM in FePt at $T=0$ is in

TABLE I. Calculated and experimental (Exp.) lattice constants (a, c), spin magnetic moments (μ), and relative energies (E) of three considered magnetic structures of MnPt and FePt shown in Fig. 1. Each energy is given with respect to that of the corresponding most stable model. As μ_{Mn} (μ_{Fe}) and μ_{Pt} atomic magnetic moments are determined within Wigner-Seitz atomic spheres, their sum may differ slightly from the total magnetic moment per formula unit cell $\mu_{\text{f.u.}}$.

	a (Å)	c (Å)	c/a	$\mu_{\text{f.u.}}$ (μ_{B} /f.u.)	$\mu_{\text{Mn,Fe}}$ (μ_{B} /at.)	μ_{Pt} (μ_{B} /at.)	E (meV/f.u.)
MnPt							
Model 1	3.99	3.70	0.93	0.00	3.80	0.00	0.0
Model 2	4.10	3.58	0.87	0.00	3.89	0.00	267.5
Model 3	4.17	3.48	0.84	4.37	3.94	0.39	293.0
Exp. ^a	4.00	3.67	0.92		4.0 ± 0.4	0.4 ± 0.4	
FePt							
Model 1	3.96	3.60	0.91	0.00	2.84	0.00	276.2
Model 2	3.90	3.66	0.94	0.00	2.94	0.00	7.2
Model 3	3.85	3.77	0.98	3.23	2.92	0.33	0.0
Exp. ^b	3.86	3.79	0.98				
Exp. ^c	3.86	3.71	0.96	3.24	2.90	0.34	
Exp. ^d					2.92 ± 0.29	0.47 ± 0.02	

^aReferences 9 and 10.

^bReference 22.

^cReference 23.

^dReference 24.

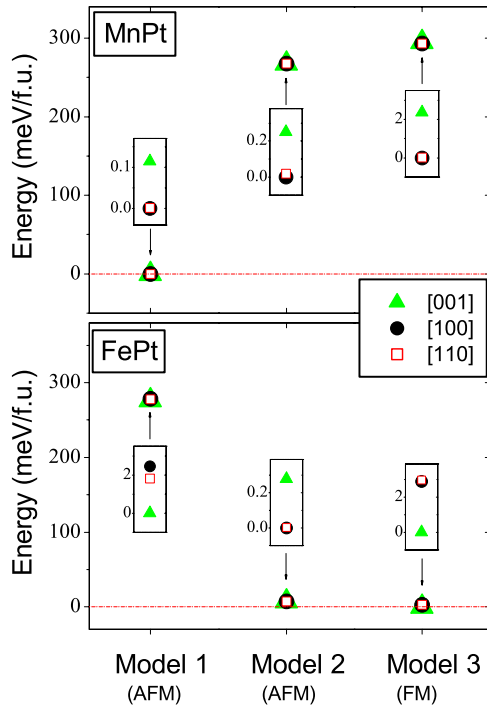


FIG. 3. (Color online) Graphical representation of relative energies from Tables I and II. The inset scales allow to distinguish the energies of different magnetic moment directions for corresponding models. The energies within the insets are calculated using spin-orbit coupling. They are given with respect to that of the most stable magnetic-moment direction for corresponding model.

accordance with results of Refs. 19 and 25. Note that, in Ref. 25, it is shown that the correct FM ground state of FePt is predicted only when the generalized gradient approximation is used due to the more accurate estimation of lattice constants. The obtained values of lattice parameters and magnetic moments of MnPt Model 1(AFM) and FePt Model 3(FM) are in good agreement with the corresponding experimental data^{8-11,22-24} and previous first-principles calculations.²⁵⁻³⁶ Pt atoms are found to have either small or negligible magnetic moments. Considering the magnetic properties of the two alloys and observing the approximate “mirror reflection” between the upper (MnPt) and lower (FePt) parts of Fig. 3, MnPt and FePt may be approximately considered as magnetic antipodes with opposite FM-AFM and in-plane/out-of-plane MCA relationships.

IV. MCA

In order to study the magnetocrystalline anisotropy, we include spin-orbit coupling and consider three possible directions ([001], [100], and [110]) of collinear atomic magnetic moments for each of three considered models shown in Fig. 1. The corresponding results for MnPt and FePt are presented in Table II and Fig. 3.

For MnPt, our calculations predict that, for all three models, the magnetic moments energetically prefer to be in the (001) plane with nonvanishing energies (0.11, 0.25, and 2.35 meV) required to orient the moments out of plane. This result, for the most stable Model 1, is in agreement with ex-

TABLE II. MnPt and FePt relative energies (E) and atom magnetic moments μ corresponding to three possible directions ([001], [100], and [110]) of collinear atomic magnetic moments for each of three considered models shown in Fig. 1. Each energy is given with respect to that of the most stable magnetic moment direction for a given model.

		Direction	E (meV/f.u.)	$\mu_{\text{Mn,Fe}}$ (μ_B /at.)	μ_{Pt} (μ_B /at.)
MnPt	Model 1	[001]	0.114	3.78	0
		[100]	0	3.78	0
		[110]	0.001	3.78	0
	Model 2	[001]	0.250	3.89	0
		[100]	0	3.89	0
		[110]	0.019	3.89	0
	Model 3	[001]	2.350	3.94	0.39
		[100]	0	3.94	0.39
		[110]	0.005	3.94	0.39
FePt	Model 1	[001]	0	2.82	0
		[100]	2.460	2.82	0
		[110]	1.805	2.81	0
	Model 2	[001]	0.280	2.94	0
		[100]	0	2.94	0
		[110]	0.003	2.93	0
	Model 3	[001]	0	2.91	0.34
		[100]	2.900	2.92	0.34
		[110]	2.990	2.91	0.34

perimental data of Ref. 10 but contrary to those of Refs. 8, 9, and 11. However, in Refs. 8, 9, and 11, transitions from out-of-plane to in-plane magnetic orientation are observed on increase of either temperature or Pt composition (immediately above equiatomic $L1_0$ stoichiometry). Such experimental sensitivity of MCA to the change in composition is consistent with our comparatively small (~ 0.1 meV/f.u.) theoretical MCA value. Moreover, the small calculated energy difference is sensitive to the details of first-principles calculations. For example, a calculation within linear muffin-tin orbital- (LMTO-) atomic sphere approximation (ASA) (neglecting the Pt magnetic moment) gives 0.51 meV/f.u. for the same MCA.²⁶

In Ref. 32, the MCA of MnPt Model 3 (FM) is calculated within FP-LMTO. But in contrast to our complete atomic relaxation, they consider fixed lattice parameters taken from experimental data for AFM MnPt. Correspondingly, the MCA values which they obtain have opposite sign and higher absolute value compared to ours. This may demonstrate that how important is the choice of lattice parameters for MCA calculation.

MnPt in-plane MCA energies ($[100]$ vs $[110]$) are found to be very small (< 0.01 meV/f.u.) for Models 1 and 3. Our calculations probably do not have sufficient accuracy to resolve such small differences. Thus it is difficult to determine the energetically preferred direction in the magnetic moments. For Model 2, the in-plane MCA energy is about 0.02 meV/f.u. and the preferred direction is $[100]$. Such an energy difference is also small and near the limits of our accuracy.

For FePt, the in-plane ($[100]$ vs $[110]$) MCA is nonvanishing for Model 1 with $[110]$ the preferred magnetic moment direction. For Models 2 and 3, the calculated in-plane MCA is too small to provide a reliable value. The out-of-plane MCAs are the largest (2–3 meV/f.u.) for Models 1 and 3 with $[001]$ the preferred magnetic-moment direction. For Model 2, the out-of-plane MCA energy is significantly higher so in-plane orientation of the magnetic moments is preferred. The obtained out-of-plane MCA energy of the ferromagnetic phase (Model 3) is in good agreement with previous first-principles calculations^{27–33,35–39} (for a comparison, see Table I in Ref. 35). The factor 2–3 difference between first principles and experimental MCA may be attributed to imperfect chemical order in experimental samples^{35,38} or to limitations of DFT-GGA.

V. DENSITY OF STATES

The spin-polarized total and angular momentum projected densities of states (TDOS and PDOS, respectively) for the three considered models of MnPt and FePt are shown in Fig. 4 (top two panels). The TDOS topologies are similar for MnPt and FePt, so that the rigid-band model is roughly valid. Correspondingly, the one electron difference between Mn and Fe is approximately reflected in a small increase in the Fermi energy between MnPt and FePt. The obtained DOS for Model 3 of FePt is in good agreement with corresponding results of Refs. 25, 28, and 32.

For both FePt and MnPt, an obvious characteristic of Model 1 (AFM) is that it has an extremely deep TDOS mini-

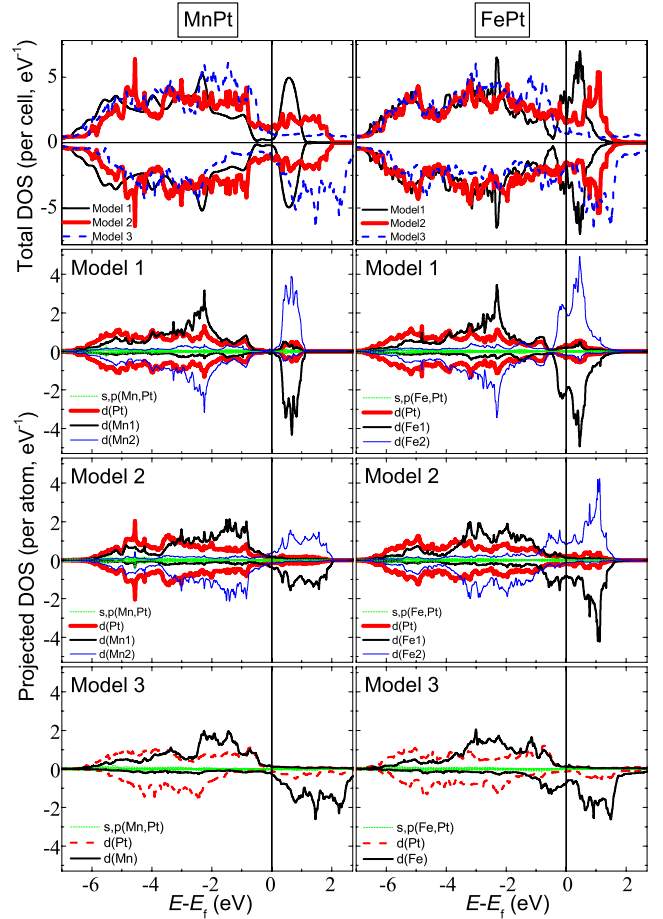


FIG. 4. (Color online) Density of states projected by spin (top panel) and by spin, angular momentum, and site (bottom three panels) for the three models of MnPt and FePt depicted in Fig. 1. E_f is the Fermi energy.

mum or “pseudogap” near the Fermi energy. For MnPt, the minimum is right at Fermi energy, while, for FePt, it is just below the Fermi energy. This can be understood by referring to Table I.

On average, the Pt d states are substantially lower in energy than the Mn d states because Pt has three more valence electrons per atom than Mn. The Pt d states are also somewhat lower in energy (on average) than the d states of Fe where the difference is two electrons per atom (see also PDOS in Fig. 4).⁴⁰ For the antiferromagnetic models, Pt has no moment so there are five electrons per Pt atom per spin channel. On the other hand, the Mn atoms have a moment of approximately 4 and the Fe atoms have a moment of approximately 3. This means that both the Mn and Fe atoms have approximately 5.5 electrons in the spin channel that is locally majority while they have 1.5 and 2.5 electrons, respectively, in the channel that is locally minority. For simplicity, we ignore interatomic charge transfer which we believe to be small in these alloys, and in any event, difficult to define unambiguously.

The implication of these electron counts is that the d states for the locally majority Mn or Fe atoms are approximately degenerate with (or even slightly lower than) the d states of Pt while the locally minority d states on the Mn and

Fe are substantially higher in energy. Thus, we can see that for Model 1, the Mn and Fe d states corresponding to the local minority spin channel form very narrow bands (mostly near and above E_F) because such d states have no neighbors of similar energy for the same channel with which to hybridize. Mn and Fe minority d states are broader for Models 2 and 3 because they can hybridize with the same states of four neighbors in (001) plane.

One feature that needs additional explanation is the striking pseudogap for model 1 which has also been seen in previous electronic-structure calculations⁴¹ for MnPt. Supporting experimental evidence has also been reported.⁴² A similar pseudogap is predicted in NiMn.⁴³ It is likely that the deep pseudogap contributes to the relative stability of Model 1 for MnPt since for this material (and for NiMn) it occurs at the Fermi energy.

We expect to explain the pseudogap in a substantially wider context elsewhere.⁴⁴ Its existence can be understood in this instance by realizing that for the Mn d states that are locally minority all nearest neighbors have d states that are substantially lower in energy. The energy shifts due to interactions between the Mn-locally minority d states and these neighbors take the form $\Delta = w^2 / (E_{Mn\downarrow} - E_d)$ where w represents the interaction between these d states, $E_{Mn\downarrow}$ is the on-site energy of a Mn d state that is locally minority, and E_d represents one of the other d states. This interaction is always positive and so only pushes the $E_{Mn\downarrow}$ d states higher in energy. Thus five d states per four atom cell must lie higher in energy than $E_{Mn\downarrow}$. In MnPt and in FePt, this is sufficiently high that there is very little overlap with the bands derived from the d states originating on the other sites.

VI. EFFECT OF TETRAGONALITY

In order to study the effect of tetragonality on the relative energy of the models for MnPt and FePt and on their magnetic and electronic properties, we varied the tetragonality ratio c/a from 0.5 to 1. For each fixed c/a , we minimized the first-principles energy over all of the other degrees of freedom for each of the considered models. The results are presented in Figs. 5 and 6 for MnPt and FePt, respectively.

For MnPt (Fig. 5), the most stable phase changes from Model 1 to Model 2 (both AFM) at $c/a \sim 0.72$ as c/a decreases. This is approximately the value of c/a for which the structure would be B2 (CsCl) rather than $L1_0$. The MCA of Model 1 increases and changes sign from negative (in-plane) to positive (out-of-plane) as c/a increases from its equilibrium (0.928) value. On the other hand, decreasing its c/a from its equilibrium value yields a stronger in-plane MCA with a minimum in $E^{100} - E^{001}$ at $c/a \sim 0.70$.

The MCA of Model 2 slowly oscillates around zero as c/a changes (including the region of Model 2 stability at $c/a < 0.7$). As c/a decreases, the magnetic moments of Mn (in all three models) and of Pt (in Model 3) increase until reaching some maximum values. There is no magnetic moment on Pt atoms in Model 1 and 2. The transition from Model 1 to Model 2 at $c/a \sim 0.7$ results in large drop in the MCA but in only a slight change in the atomic magnetic moments. We may say that by a transition from Model 1 to Model 2, the

system maintains the low magnetic moment on Mn atoms and low MCA. Our results confirm that the tetragonality has a nonmonotonic, comparatively minor effect on MCA (in contrast to long-range order effect, see Fig. 2 in Ref. 38).

In MnPt, the FM state is not competitive with the AFM state at $T=0$ K. As tetragonality increases (c/a decreases), we may expect a change in AFM type rather than the appearance of FM order (see Fig. 5). If we assume that, in MnPt, the FM phase becomes energetically favored compared to AFM as the system becomes more cubic [similar to FePt (Ref. 19)], then this may explain the experimentally observed^{12,13} ferromagnetic phase in quenched MnPt samples.

For FePt (see Fig. 6), the most stable phase changes from Model 3 (FM) to Model 2 (AFM) at $c/a \sim 0.948$. This transition occurs very close to the global equilibrium c/a value of 0.98. The MCA changes sign with this transition (out-of-plane to in-plane). Model 2 and Model 3 are nearly degenerate. We estimate that an uniaxial pressure of 4.3 GPa is necessary to shift the system from its FM ground state ($c/a=0.98$) to a metastable AFM state ($c/a=0.94$). With further decrease in c/a , the MCA changes back to out-of-plane and reaches a maximum (within the same stable Model 2). The obtained variation of the FePt MCA of Model 3 is in good agreement with the corresponding results of Refs. 28, 35, and 39 calculated within the LMTO-ASA, FP-LMTO, and full potential local orbital methods, respectively.

Our result that, the AFM state in FePt can be achieved by a small variation in the tetragonality ratio c/a at $T=0$ K, confirms the corresponding result of Brown *et al.*¹⁹ Note, however, that we predict that the FM state is the one that is stable at $T=0$ K and low pressure. Brown *et al.*¹⁹ also have shown that ferromagnetism becomes energetically stronger than AFM at the decrease of tetragonality (i.e., at $c/a \rightarrow 1$) and/or $L1_0$ order (so, effectively, as the system becomes more cubic). This may help to explain why the AFM state in FePt is not experimentally observed at ambient temperature and pressure.

The magnetic configuration is determined by the relative direction of magnetic moments on adjacent $3d$ transition metal atoms. As the tetragonality ratio, c/a , changes, the interatomic distances and interactions also change. In Table III, we show the lattice constants and nearest-neighbor distances for three considered c/a values in both MnPt and FePt. Table III demonstrates that, with decrease in c/a , the Mn-Mn and Fe-Fe distances in the (001) plane increase considerably, while the Mn-Pt and Fe-Pt distances do not change as much. Note that, for $c/a \in [0.52-1]$, the unit-cell volume remains relatively constant for all considered models.

We also study the c/a change in PDOS corresponding to Fe and Mn atoms. We find that, for all three models of MnPt and FePt, the PDOS of the transition-metal atoms change similarly. Thus, in Fig. 7 we present the PDOS data only for the Mn atom in Model 1 of MnPt as an example. Note that our results are comparable to those obtained by the tight-binding (TB)-LMTO method in Ref. 41 (see Fig. 7 there).

These results can be understood using the simple model presented in Sec. V in which the d states of the Pt atoms and the Mn d states that are locally majority are approximately degenerate and considerably lower than the Mn d states on

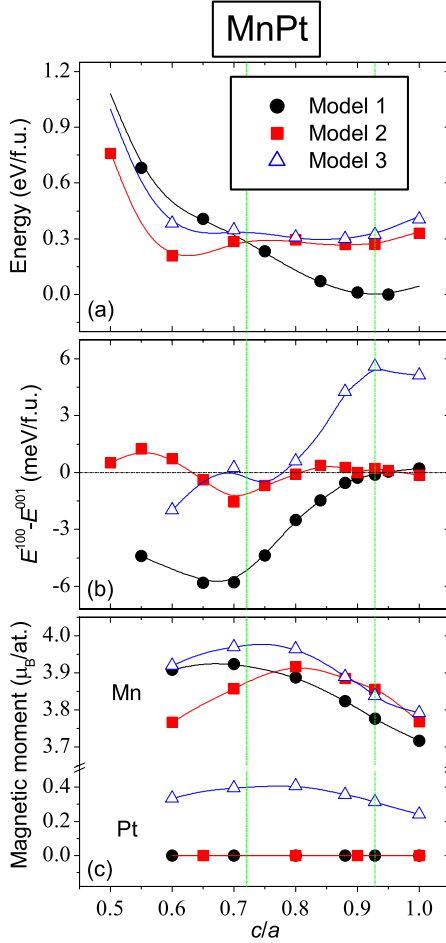


FIG. 5. (Color online) In case of MnPt, the dependencies on the tetragonality ratio c/a of (a) energies (with reference to the ground state, which is Model 1 at $c/a=0.928$); (b) out-of-plane MCAs; and (c) atom magnetic moments. The curve designations are the same for all three graph panels. Two vertical grid lines designate $c/a = 0.72$ corresponding to the change in energetic preference between Model 1 and Model 2 and the globally equilibrium $c/a=0.928$.

the locally minority Mn atoms. Let us first consider the width of the (unoccupied) minority Mn d bands. These can be seen to broaden significantly as we decrease c/a . The reason for this is that the minority Mn d states can hybridize effectively only with other minority Mn d states. In Model 1, the closest of these can be found at distance c in the (001) direction. As c is reduced these states broaden significantly. For the Mn

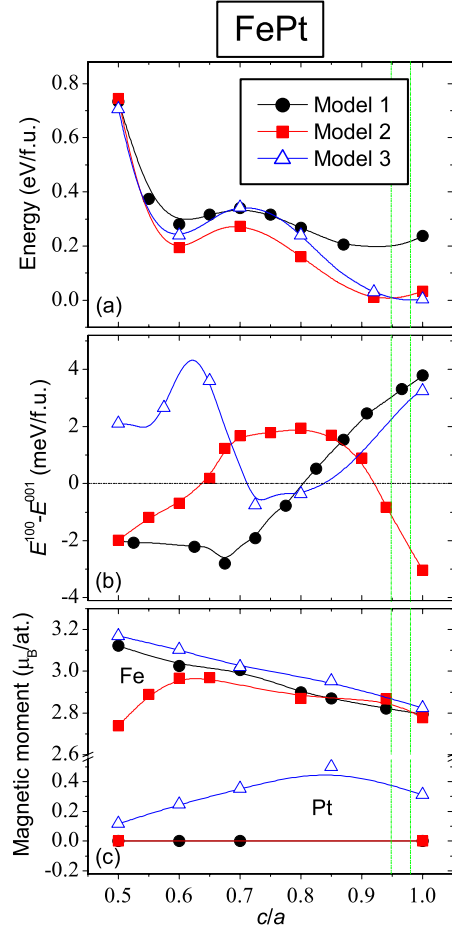


FIG. 6. (Color online) The same as in Fig. 5 but for FePt. Two vertical grid lines designate $c/a=0.948$ corresponding to the change in energetic preference between Model 3 and Model 2 and the globally equilibrium $c/a=0.98$.

majority d states, on the other hand the nearest Mn states with which to hybridize are in the plane a distance a away in Model 1. These states get further away as c/a decreases. The Mn majority d states can also hybridize with the Pt d states, however their distance does not change greatly as c/a decreases (see Table III). The net effect is that these states narrow as c/a decreases.

Because the Fermi energy of MnPt falls in the pseudogap, we speculate that it is important for understanding its phase stability. The energy of Model 1 increases with decreasing c/a because the broadening seen in Fig. 7 eliminates the

TABLE III. Lattice constants (a, c) and nearest atomic distances (d) at three different values of c/a in Model 1 of MnPt ($T=Mn$) and Model 3 of FePt ($T=Fe$). Such models are presented as they are the magnetic ground states of corresponding compounds.

	MnPt			FePt		
c/a	1	0.8	0.5	1	0.8	0.5
$a(\text{\AA})$	3.89	4.31	5.06	3.82	4.13	4.94
$c(\text{\AA})$	3.89	3.37	2.53	3.82	3.31	2.47
$d_{T-T}^{\text{in-plane}}(\text{\AA})$	2.75	3.05	3.58	2.70	2.92	3.49
$d_{T-Pt}(\text{\AA})$	2.75	2.72	2.83	2.70	2.65	2.76

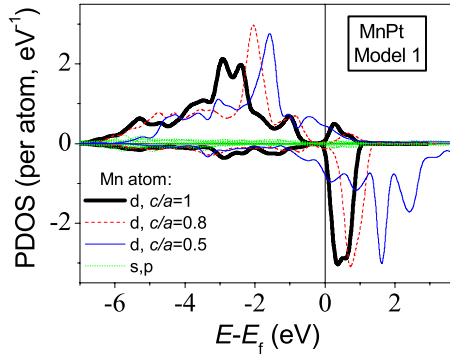


FIG. 7. (Color online) Angular momentum PDOS of Mn atom for Model 1 in case of MnPt for three different values of c/a tetragonality ratio.

Fermi energy pseudogap and its stabilizing effect. On the other hand, the energies of Models 2 and 3 are relatively insensitive to c/a .

VII. CONCLUSIONS

In this paper, we study the magnetic and electronic properties of three different spin configurations of the $L1_0$ phase (see Fig. 1) of FePt and MnPt alloys. It is found that MnPt and FePt may be approximately considered as magnetic antipodes with opposite FM-AFM and in-plane/out-of-plane MCA relationships. This is most clearly shown by almost mirror reflection between the upper (MnPt) and lower (FePt) parts of Fig. 3. Namely, Model 1 (AFM) with in-plane spins is the most stable magnetic configuration whereas Model 3 (FM) with out-of-plane spins is the most unstable one in MnPt. In FePt, the situation is exactly opposite.

The out-of-plane MCA of MnPt is more than an order of magnitude less (~ 0.1 meV) than that of FePt (~ 2.9 meV) in the corresponding magnetic ground states. Such a small value for MnPt explains the experimentally observed controversy and sensitivity of the MCA to changes in composition and temperature.^{8–11} Besides, being small, the out-of-plane MCA of MnPt is sensitive to the details of first-principles calculations.²⁶ The out-of-plane MCA of FePt is in good agreement with previous first-principles calculations.^{27–33,35–39} The factor 2–3 difference between first principles and experimental FePt MCA may be attributed either to imperfect chemical order in experimental samples,^{35,38} deficiencies in density functional theory or both. In all considered cases, the in-plane MCA is found to be very small (near the limits of our accuracy).

The obtained values of lattice parameters and magnetic moments of MnPt and FePt magnetic ground states are in

good agreement with the corresponding experimental data^{8–11,22–24} and previous first-principles calculations.^{25–36} Pt atoms are found to have either small (0.39 for MnPt, 0.34 for FePt for Model 3) or negligible magnetic moments (Models 1 and 2).

Our calculations predict that the AFM state in FePt can be achieved by a small variation of the tetragonality ratio c/a (from 0.98 to 0.94, see Table I and Fig. 5), confirming the corresponding result of Brown *et al.*¹⁹ Brown *et al.*¹⁹ also have shown that ferromagnetism becomes energetically stronger than AFM at the decrease in tetragonality (i.e., at $c/a \rightarrow 1$) and/or $L1_0$ order (so, effectively, as the system becomes more cubic). This may help to explain why the AFM state in FePt is not experimentally observed at ambient temperature and pressure.

In MnPt, the FM state is not competitive with the AFM state at $T=0$ K. On increasing of tetragonality ratio c/a , we may expect a change in AFM type rather than appearance of FM order (see Fig. 5). If we assume that, in MnPt, the FM phase becomes energetically favored compared to AFM when the $L1_0$ order is decreased [similar to FePt (Ref. 19)] then this may explain the experimentally observed^{12,13} ferromagnetic phase in quenched MnPt samples.

Our results confirm that the tetragonality has a nonmonotonic, comparatively minor effect on MCA (in contrast to the effect of long-range order³⁸). The magnetic moment as a function of tetragonality usually has one maximum. Generally, we observe that by transitions between different magnetic configurations, the systems maintain the low magnetic moments and MCA.

The DOS topologies are quite similar for MnPt and FePt so that the rigid-band model is roughly valid. Correspondingly, the electron difference between Mn and Fe is approximately reflected in the relative location of the Fermi energy. We find that, in MnPt, the pseudogap is observed near the Fermi energy in all three considered models. Such effect is observed experimentally⁴² and theoretically (TB-LMTO).⁴¹ In FePt, the narrow pseudogap is calculated only in Model 1 (AFM).

We find that the valence band consists mainly of d electrons. The d states for the locally majority Mn or Fe atoms are approximately degenerate with (or even slightly lower than) the d states of Pt while the locally minority d states on the Mn and Fe are substantially higher in energy.

ACKNOWLEDGMENTS

This research was supported by the National Science Foundation under Grants No. NSF-DMR-MRSEC 0213985 and No. NSF-ECS-0529369.

*Present address: Duke University, Durham, NC 27708, USA.

†wbutler@mint.ua.edu

¹R. F. C. Farrow, R. F. Marks, S. Gider, A. C. Marley, S. S. P. Parkin, and D. Mauri, *J. Appl. Phys.* **81**, 4986 (1997).

²M. F. Toney, M. G. Samant, T. Lin, and D. Mauri, *Appl. Phys. Lett.* **81**, 4565 (2002).

³M. J. Carey, A. B. Banful, L. Folks, B. A. Gurney, R. F. C. Farrow, and A. J. Kellock, *Appl. Phys. Lett.* **84**, 3097 (2004).

- ⁴D. Weller, A. Moser, L. Folks, M. E. Best, L. Wen, M. F. Toney, M. Schwickert, J.-U. Thiele, and M. F. Doerner, *IEEE Trans. Magn.* **36**, 10 (2000).
- ⁵S. Sun, C. B. Murray, D. Weller, L. Folks, and A. Moser, *Science* **287**, 1989 (2000).
- ⁶H. Zeng, J. Li, J. P. Liu, Z. L. Wang, and S. Sun, *Nature (London)* **420**, 395 (2002).
- ⁷*Binary Alloy Phase Diagrams*, 2nd ed., edited by T. B. Massalski, H. Okamoto, P. K. Subramanian, and L. Kacprzak (American Society for Metals, Metals Park, OH, 1990).
- ⁸A. F. Andresen, A. Kjekshus, R. Mollerud, and W. B. Pearson, *Philos. Mag.* **11**, 1245 (1965).
- ⁹E. Krén, C. Kádár, L. Pál, J. Sólyom, P. Szabó, and T. Tarnóczy, *Phys. Rev.* **171**, 574 (1968).
- ¹⁰C. S. Severin, C. W. Chen, and C. Stassis, *J. Appl. Phys.* **50**, 4259 (1979).
- ¹¹H. Hama, R. Motomura, T. Shinozaki, and Y. Tsunoda, *J. Phys.: Condens. Matter* **19**, 176228 (2007).
- ¹²C. W. Chen and R. W. Buttry, *Magnetic bubbles—for the non-specialist*, AIP Conf. Proc. Vol. 24 (AIP, New York, 1975), p. 437.
- ¹³C. S. Severin and C. W. Chen, *J. Appl. Phys.* **49**, 1693 (1978).
- ¹⁴K. Shimoyama, T. Kato, S. Iwata, and S. Tsunashima, *IEEE Trans. Magn.* **35**, 3922 (1999).
- ¹⁵T. Kume, Y. Sugiyama, T. Kato, S. Iwata, and S. Tsunashima, *J. Magn. Magn. Mater.* **272-276**, Supplement 1, E827 (2004).
- ¹⁶R. Wirths, P. Runow, and H. W. Schöpgens, *Phys. Status Solidi A* **33**, 135 (1976).
- ¹⁷G. E. Bacon and J. Crangle, *Proc. R. Soc. London, Ser. A* **272**, 387 (1963).
- ¹⁸O. A. Ivanov, L. V. Solina, V. A. Demshina, and L. M. Magat, *Fiz. Met. Metallovd.* **35**, 92 (1973).
- ¹⁹G. Brown, B. Kraccek, A. Janotti, T. C. Schulthess, G. M. Stocks, and D. D. Johnson, *Phys. Rev. B* **68**, 052405 (2003).
- ²⁰Y. Wang and J. P. Perdew, *Phys. Rev. B* **44**, 13298 (1991).
- ²¹G. Kresse and J. Furthmüller, *Comput. Mater. Sci.* **6**, 15 (1996); *Phys. Rev. B* **54**, 11169 (1996); G. Kresse and D. Joubert, *ibid.* **59**, 1758 (1999).
- ²²*Pearson's Handbook of Crystallographic Data for Intermetallic Phases*, edited by P. Villars and L. D. Calvert (American Society for Metals, Metals Park, OH, 1985).
- ²³J. Lyubina, I. Opahle, M. Richter, O. Gutfleisch, K.-H. Müller, L. Schultz, and O. Isnard, *Appl. Phys. Lett.* **89**, 032506 (2006).
- ²⁴C. Antoniak and M. Farle, *Mod. Phys. Lett. B* **21**, 1111 (2007).
- ²⁵J. M. MacLaren, R. R. Duplessis, R. A. Stern, and S. Willoughby, *IEEE Trans. Magn.* **41**, 4374 (2005).
- ²⁶R. Y. Umetsu, A. Sakuma, and K. Fukamichi, *Appl. Phys. Lett.* **89**, 052504 (2006).
- ²⁷G. H. O. Daalderop, P. J. Kelly, and M. F. H. Schuurmans, *Phys. Rev. B* **44**, 12054 (1991).
- ²⁸A. Sakuma, *J. Phys. Soc. Jpn.* **63**, 3053 (1994).
- ²⁹I. V. Solov'ev, P. H. Dederichs, and I. Mertig, *Phys. Rev. B* **52**, 13419 (1995).
- ³⁰P. M. Oppeneer, *J. Magn. Magn. Mater.* **188**, 275 (1998).
- ³¹I. Galanakis, M. Alouani, and H. Dreyssé, *Phys. Rev. B* **62**, 6475 (2000).
- ³²P. Ravindran, A. Kjekshus, H. Fjellvåg, P. James, L. Nordström, B. Johansson, and O. Eriksson, *Phys. Rev. B* **63**, 144409 (2001).
- ³³A. B. Shick and O. N. Mryasov, *Phys. Rev. B* **67**, 172407 (2003).
- ³⁴A. Kashyap, R. Skomski, A. K. Solanki, Y. F. Xu, and D. J. Sellmyer, *J. Appl. Phys.* **95**, 7480 (2004).
- ³⁵T. Burkert, O. Eriksson, S. I. Simak, A. V. Ruban, B. Sanyal, L. Nordström, and J. M. Wills, *Phys. Rev. B* **71**, 134411 (2005).
- ³⁶T. Oda and A. Hosokawa, *Phys. Rev. B* **72**, 224428 (2005).
- ³⁷S. Ostanin, S. S. A. Razee, J. B. Staunton, B. Ginatempo, and E. Bruno, *J. Appl. Phys.* **93**, 453 (2003).
- ³⁸J. B. Staunton, S. Ostanin, S. S. A. Razee, B. Gyorffy, L. Szunyogh, B. Ginatempo, and E. Bruno, *J. Phys.: Condens. Matter* **16**, S5623 (2004).
- ³⁹J. Lyubina, I. Opahle, K.-H. Müller, O. Gutfleisch, M. Richter, M. Wolf, and L. Schultz, *J. Phys.: Condens. Matter* **17**, 4157 (2005).
- ⁴⁰However, it is necessary to include the effects of spin polarization.
- ⁴¹A. Sakuma, *J. Phys. Soc. Jpn.* **69**, 3072 (2000).
- ⁴²R. Y. Umetsu, K. Fukamichi, and A. Sakuma, *J. Appl. Phys.* **91**, 8873 (2002).
- ⁴³A. Sakuma, *J. Magn. Magn. Mater.* **187**, 105 (1998).
- ⁴⁴W. H. Butler and C. K. A. Mewes (unpublished).